Structure of lengenbachite: A high-resolution transmission electron microscope study

TIMOTHY B. WILLIAMS*

The Institute for Materials Research, Tohoku University, Katahira 2-1-1, Sendai 980, Japan

ALLAN PRING

The South Australian Museum, North Terrace, Adelaide, S.A. 5000, Australia

ABSTRACT

High-resolution transmission electron microscopy and electron diffraction have been used to examine the structure of lengenbachite, of approximate composition $Pb_6As_4(Ag,Cu)_2S_{13}$. The structure deduced consists of a semicommensurate intergrowth of a pseudotetragonal layer (T), a sheared four-atom-thick {100} PbS-like slice, and a slightly distorted five-atom-thick pseudo-orthohexagonal {111} M_2S_3 slice (O). Both layer types contain Pb and As atoms in cation sites, giving layer stoichiometries of $T = (Pb,As)_4S_4$ and $O = (As,Pb)_2S_3$. The structure is in agreement with the cell geometries and compositions proposed by earlier workers. The relationships with the structures of cylindrite and "franckeites" are also discussed.

INTRODUCTION

Lengenbachite, $\sim Pb_6As_4(Ag,Cu)_2S_{13}$, from its only known occurrence at Binntal in the Swiss Dolomites, was described by Solly (1905). Subsequently, several workers (Nuffield, 1944; Nowacki, 1968; E. Makovicky and E. S. Leonardsen, in Makovicky and Hyde, 1981) have attempted X-ray structure determinations, but with little success. The mineral is layered, with a perfect {100} cleavage, and is relatively malleable; these properties render specimen preparation for single-crystal work extremely difficult and for powder examination probably impossible. In addition to this problem, the crystals are heavily twinned, obscuring the true value of the angle β, and considerable stacking disorder has also been reported (E. Makovicky and E. S. Leonardsen, in Makovicky and Hyde, 1981). The geometric crystallographic data of Makovicky and Leonardsen are summarized in Table 1. These data indicate that the structure consists of two layers, a pseudotetragonal (but triclinic) layer T, alternating with a pseudo-orthohexagonal layer, O (also triclinic).[1] The common interlayer parameters b and c are semicommensurable, $3b_O = 2b_T = 11.68$ Å and $12c_T = 11c_O = 70.16$ Å, thus defining the common mesh and hence the true cell (t) of Table 1, as the two-layer-pair repeat and common stacking directions give common parameters $a = 18.45$ Å for the three cells. A schematic illustration of the real-space (100) unit mesh for the subcells is given in Figure 1. This sort of semicommensurate match is very

similar to those in the layered Pb-Sn-Sb-Fe-S minerals cylindrite and the "franckeites," which have recently been successfully studied by high-resolution transmission electron microscopy (HRTEM) (Williams and Hyde, 1988).

Considering the apparent structural similarities between these three families of sulfosalt minerals and the results obtained from the study of cylindrite and franckeite, an HRTEM study of lengenbachite seemed to be worthwhile. A preliminary account of this work was presented at the 14th IUCr meeting in August 1987.

EXPERIMENTAL DETAILS

Bladelike crystal fragments of lengenbachite about 5–10 mm in length were kindly provided by the Naturhistorisches Museum, Bern, and the British Museum (Natural History) (BM 87133). They were prepared for examination in the electron microscope in two ways. For the [100] zone, i.e., normal to the layering, the cleavage was utilized to facilitate ultrasonically fragmenting the material in alcohol, and a drop of the resulting suspension was placed on a standard holey-carbon specimen-support grid. For the other principal zones [010] and [001], oriented thin sections were milled with an Ar-ion beam to electron transparency.

For the [100] zone fragments, a JEOL 200CX electron microscope fitted with a high-resolution double-tilt top-entry stage ($C_s = 1.2$ mm) was used. The ion-milled samples were examined in a Philips EM430T ("twin") machine equipped with a side-entry double-tilt stage ($C_s = 2.0$ mm) and operated at 300 kV. The point-to-point resolutions and optimum (Scherzer) defoci of the two machines in the above configurations were 2.49 Å and -670 Å, and 2.35 Å and -770 Å for the JEOL and Philips instruments, respectively. Simulation of high-resolution images of the [010] zone axis was performed by the conventional multislice method, using local programs based on routines by G. R. Anstis (pers. comm.). Arrays of 512×32 points (7281 "beams") were used in the calculation of Fourier coefficients and the multislice iteration. The slice thickness was 2.5 Å, and images were calculated for foils from 10 to 50 Å in thickness in 10-Å increments at foci

---

* Present address: Anorganische Chemisches Institut, Universität der Zürich, 8057 Zürich, Switzerland.

[1] Note a difference in notation: Makovicky and Hyde (1981) suggested H to indicate a pseudohexagonal layer type. For consistency with the earlier electron-microscope study of cylindrite and franckeite (Williams and Hyde, 1988; see also Otero-Diaz et al., 1985), we retain the O = orthohexagonal notation used by them.

TABLE 1. Unit-cell parameters for lengenbachite (from E. Makovicky and E. S. Leonardsen, in Makovicky and Hyde, 1981)

Cell type	a (Å)	b (Å)	c (Å)	$\alpha = \beta$ (°)	γ (°)
T	18.45	5.84	5.85	90.0	91.01
O	18.45	3.90	6.38	90.0	91.01
t	18.45	11.68	70.16	90.0	91.01

Note: Cell contents $Pb_{180}As_{120}(Ag,Cu)_{60}S_{390}$, calculated from Huchinson (1907). Parameters are listed for the subcells, pseudotetragonal T, pseudo-orthohexagonal O, and the true cell, t, respectively. Other X-ray studies have given $a' = 2a = 37.0$ Å, and $\beta = 92.5°$ (Nowacki, 1968) or $\beta = 94°$ (Nuffield, 1944).

Fig. 1. Schematic representation of the unit meshes for the T (heavy lines) and O (light lines) subcells of lengenbachite in the common (100) plane. Both subcells are centered.

from -100 to -1000 Å in 100-Å steps. The experimental and calculated images were compared visually. A number of T-layer modifications varying from PbS-like to a SnS (layered structure) type were tried. The metal sites of the T and O layers were occupied either by Pb (T layer) and As (O layer) or by mixed Pb and As in both layers (contrast the Bi and Pb occupancy of the structurally related layers in cannizzarite; Matzat, 1979).

RESULTS

Electron-diffraction patterns from the [100] zone (Fig. 2a) graphically illustrate the intralayer matching of the two subcells, which is indeed both perfect and fixed at the values noted above. No variation in the matching was observed in any of the fragments examined.

In many-beam images (Fig. 2b), the 11.68- and 70.16-Å true cell periods can be seen, as well as finer detail with a separation corresponding to half the c parameter of the O subcell, ~ 3.2 Å. However, images of layered structures normal to the layers are generally not directly interpretable (i.e., by assuming that the image contrast simply reflects the projected atomic structure—commonly known as the projected-charge-density approximation) if the layers are semi- or incommensurable, as moiré interference results. In this case, the use of computer-simulation methods may also be of limited usefulness (see, e.g., Holladay and Eyring, 1986).

Unfortunately, the [001] zone is also unfavorable for structure determination, owing to the long-period **c** match: a one-unit-cell-thick foil is ~ 70 Å thick and hence probably not interpretable using current electron-optical theories. As can be seen below, there is a further complication in this orientation, owing to corrugation of the layers. Nevertheless, a simplistic interpretation of the lattice image in Figure 3b suggests that the layers are straight in the **b** direction, and also the layer-pair repeat of ~ 18.5 Å is clearly visible. High-quality images could not be obtained from this zone, and there is evidence that the samples were damaged during the thinning process, as the image quality deteriorates toward the thin edge. The selected-area diffraction pattern (Fig. 3a) illustrates the match of the $2b_T$ to $3b_O$ subcells.

The [010] zone (parallel with the layers) is the most informative section. A measure of how much information there is can be seen in the complex diffraction pattern of Figure 4a, which is indexed using the cells of Table
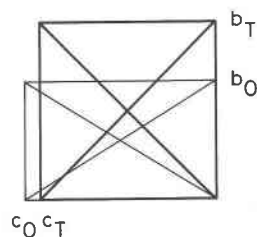
1. Many-beam images (Fig. 4b) directly show the layering and show furthermore that the layers are not flat but smoothly corrugated by a ± 0.8-Å displacement parallel with **a** and with a wavelength of $\lambda \approx 35$ Å, corresponding to half the true cell repeat in the **c** direction. Similar corrugation, though not nearly so well developed, has also been observed in lattice images of cylindrite and "franckeite" (Williams and Hyde, 1988), as well as some layered nonsulfide minerals such as antigorite (Thomas et al., 1978). Figure 5 shows the extensive microtwinning on the {100} plane reported by the earlier workers, and with the exception of thinning-induced damage, no other alterations, such as the stacking disorder reported by Makovicky and Leonardson (in Makovicky and Hyde, 1981), were seen. A trial structure was deduced from the earlier X-ray data of Makovicky and Leonardson, the electron-optical data, and the presumed relationships between this structure and those of cylindrite and the franckeites. The trial structure consists of two layer types, which alternate in the **a** direction. One is a slightly distorted (111) PbS-like slab, two octahedra-thick ("$2O$") or five atomic layers thick, that contains $(As,Pb)_4S_6$: the pseudo-ortho-hexagonal O layer. The other is a sheared (100) slab like the layers of PbS or SnS (hertzenbergite) (four atomic layers thick): the pseudotetragonal T layer ("$1T$").[2] In the common (100) plane, the subcell b and c parameters are semicommensurate. If the layers were derived from perfect archetypes, with $b_T/c_T = 1.0$ and $b_O/c_O = 1/\sqrt{3} \approx 1/1.732$, i.e., a perfectly tetragonal T layer and a perfectly hexagonal O layer, the layers would be incommensurable in both interlayer directions, since $b_T/b_O = \sqrt{2}$, and $c_T/c_O = \sqrt{(2/3)}$. However, neither layer type is derived from a perfect PbS parent structure; in the real structure these ratios are slightly altered and so become integral: $b_T/b_O = 3/2$ and $c_T/c_O = 11/12$.

The layer stoichiometries are $12Pb_{16}S_{16}$ (T layer) and $11As_{12}S_{18}$ (O layer), giving a composition $Pb_{192}As_{132}S_{390}$, almost iso-electronic with $Pb_{180}(Ag_{36}Cu_{24})As_{120}S_{390}$, the formula calculated from the analysis of Huchinson (1907).

---

[2] SnS can be considered to be derived from a perfect PbS or NaCl archetype mainly by slip or shear of alternate slabs two atomic layers thick and parallel to $[101]_{SnS}$. In this respect, the structure of SnS (hertzenbergite) is layered, but that of PbS is not.
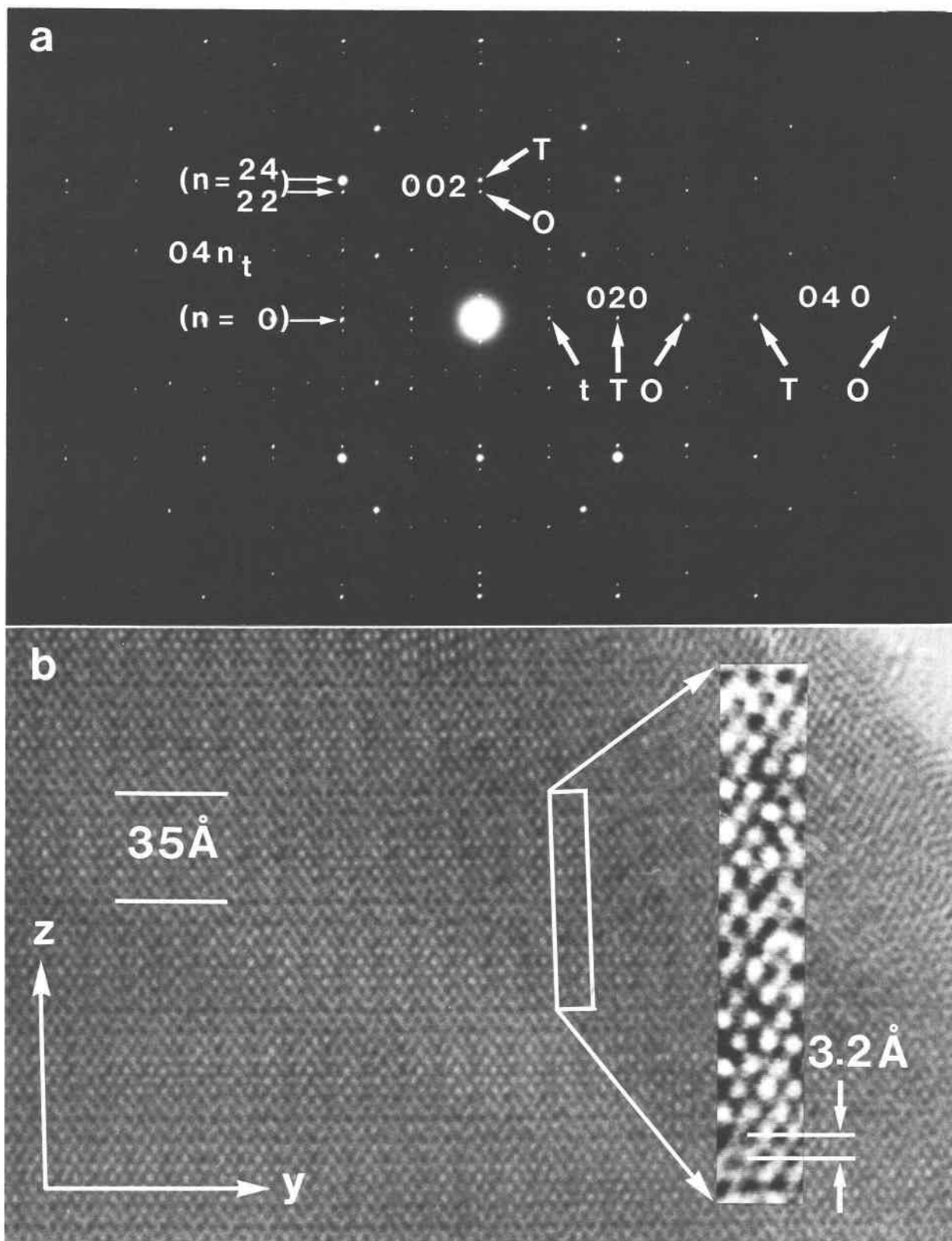
Fig. 2. (a) Selected-area electron-diffraction pattern from the [100] zone of lengenbachite. Reflections corresponding to the pseudotetragonal (T) and pseudo-orthohexagonal (O) subcells and the true cell (t) are indicated, although in such a structure the "subcell" reflections do not exist as such and appear as intense true-cell reflections. (b) A high-resolution image from the [100] zone, with the true cell outlined and enlarged.
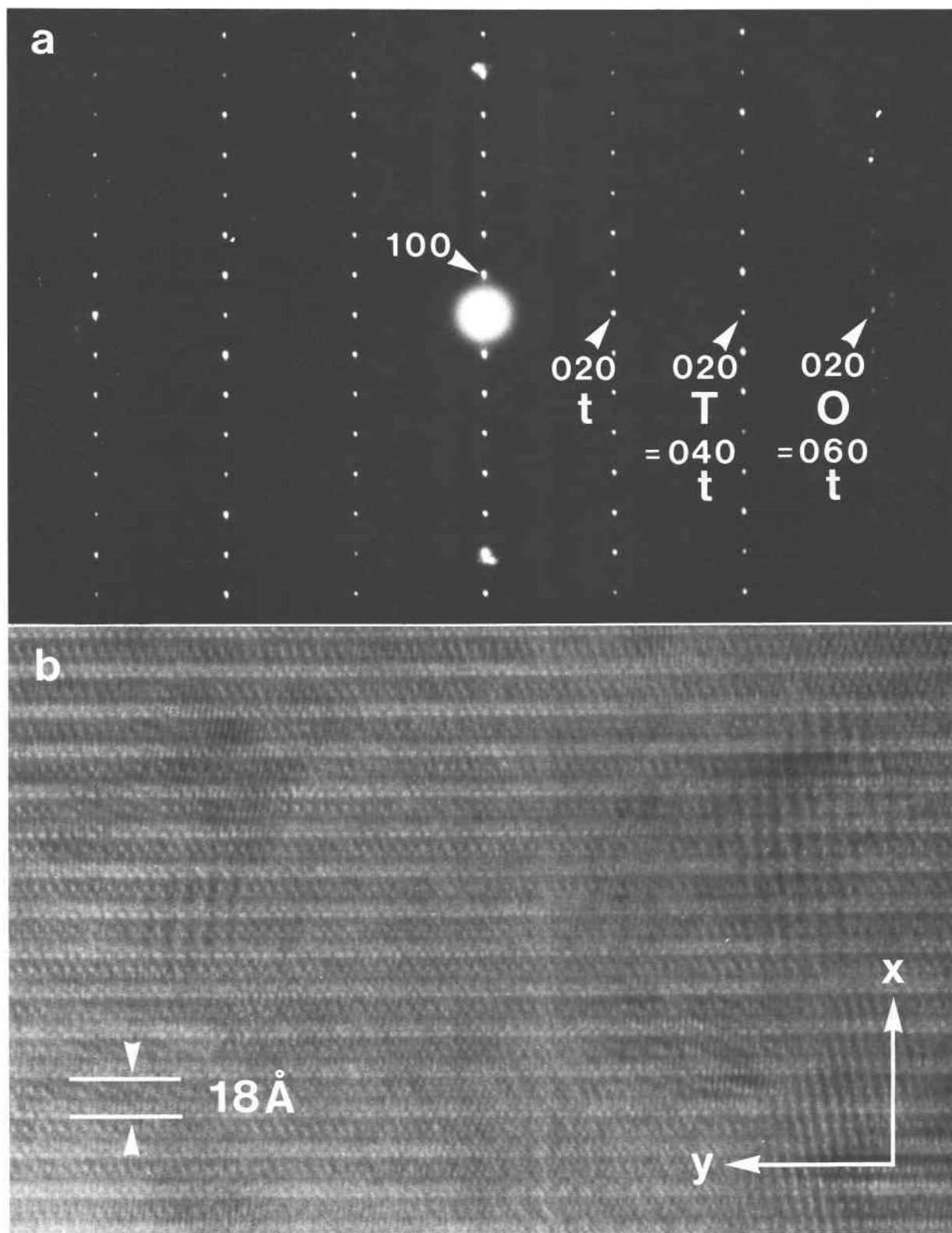
Fig. 3. Electron-diffraction pattern (a) and lattice image (b) from the [001] zone. Samples in this orientation were prepared by Ar-ion-beam milling the appropriate thin sections of single crystals. The diffraction pattern shows the layer repeat a = 18.45 Å and a perfect 2:3 subcell b match. Broad fringes in the image correspond to apparently flat layers with an ~18.45-Å separation. Disorder in the [001] zone images increases toward the thin edge of the foil and hence probably results from the thinning process.

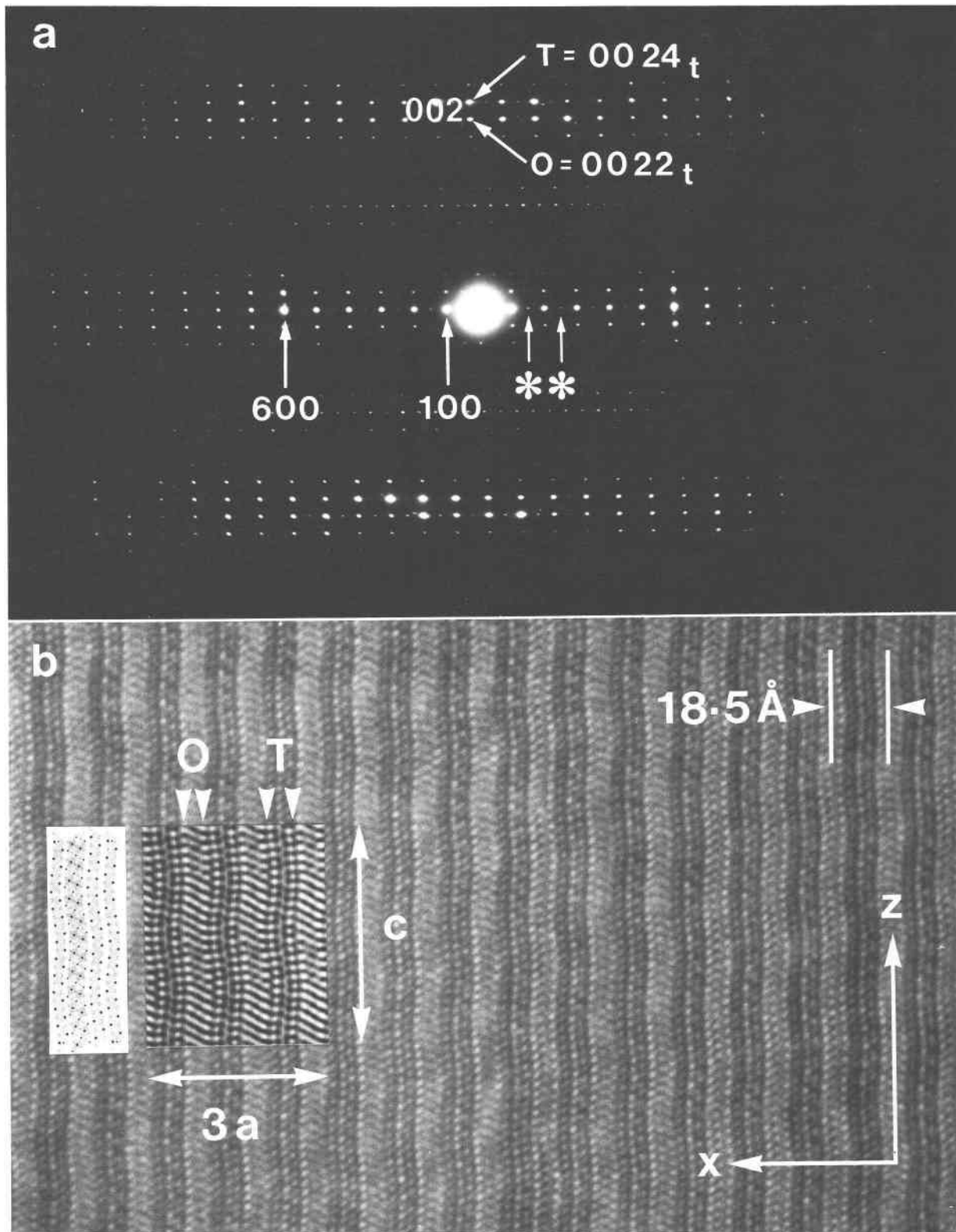Fig. 4. (a) Complex electron-diffraction pattern from the [010] zone, indexed using the three cells T, O, and t. Strong reflections from the 18.45-Å-thick layer pair with weaker intermediate reflections (*) suggests some compositional ordering (cf. the $a = 37$ Å variant reported by Nowacki, 1968); these weaker reflections were observed to a greater or lesser degree in all the diffraction patterns from this zone. (b) [010] zone axis high-resolution image and inset calculated image for a foil 20 Å thick at the optimum (Scherzer) defocus. The periodic layer corrugation is readily seen. The calculated image and hence the experimental image also are effectively structure images, i.e., dark regions correspond to high projected atomic potential. For comparison, a drawing of the structure used in the image calculations is shown inset.
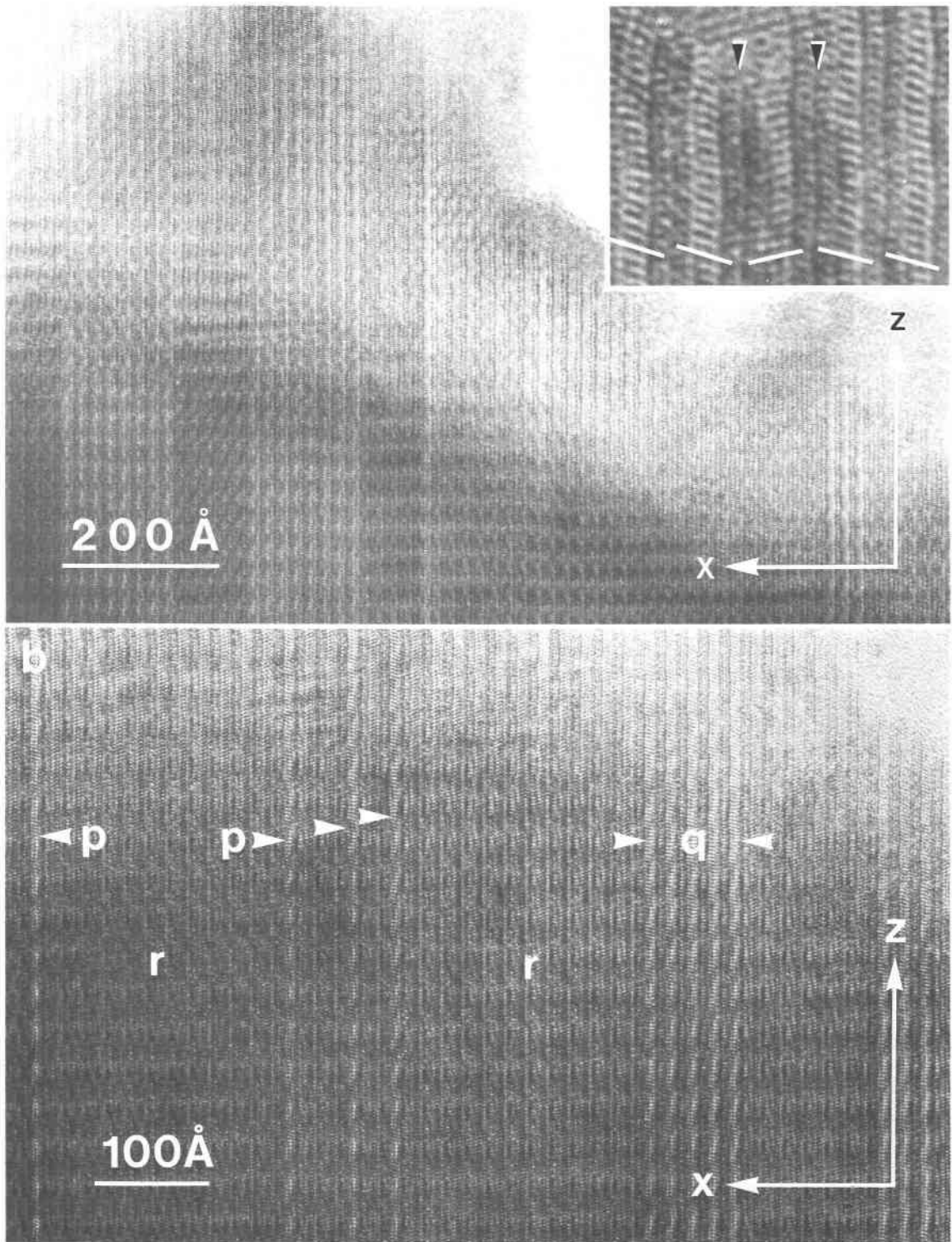
Fig. 5. [010] zone-axis lattice images showing the high density of twin planes frequently encountered in lengenbachite. (a) The light and dark gray bands are twins of each sort, with image contrast resulting from slight misorientation of one or the other twin owing to the angle γ. The inset shows the twinning (two twin planes have arrows) at high magnification, near to the thin edge of the foil. Short lines show the mirror-related O-layer orientations in the twins. Emission X-ray analyses obtained in the transmission microscope showed no compositional difference between the twinned and untwinned regions. (b) Isolated (p) and a group (q) of twins in "normal" material (r) are indicated. Twinning in this mineral occurs on the (100) cleavage plane as a result of two energetically similar but divergent layer-stacking arrangements.

The structural model, refined by comparison of structural images and computed images produced by the multislice method, is shown in Figure 6. A full list of the atomic coordinates is available.[3]

DISCUSSION

The best match between the experimental structure image of Figure 4b, which was taken from a very thin part of the crystal at close to the optimum defocus setting, and calculated images was achieved by using a slightly sheared SnS-like T layer, rather than the perfect (i.e., PbS- or NaCl-like) layer tried initially. With the thin foils used in the image calculations, very little variation of images with the foil thickness over the range of 10 to 50 Å was expected, and this was observed in practice. Variation of the focus parameter was found to have a large effect on the resulting images.

Our attempts to determine the degree of As-Pb mixing in the layers (and such mixing almost certainly occurs in this mineral) from the image-simulation results were equivocal. The calculated image of Figure 4b assumed pure PbS T layers and As_2S_3 O layers. The use of a model structure with 20% of the T-layer cation sites occupied at random by As, and 30% of the O-layer cation sites occupied by Pb (thus corresponding approximately to the Pb-Bi mixing in cannizzarite; Matzat, 1979) resulted in visually similar contrast for the two sorts of layers. Also, the proposed model has layers that are uniformly corrugated by a sinusoidal function, displacing all the atoms normal to the (100) plane. Although the resulting computed images are visually similar to those obtained experimentally, there remains some doubt as to the accuracy or uniformity of the corrugation function. These aspects of the structure refinement must await images of higher quality, including a through-focus series of images from the same crystal, and the detailed processing of suitable structure images to allow refinement of the corrugation and local layer structures.

The double-layer structure of lengenbachite clearly relates the mineral to the Pb-Sn–based sulfosalts cylindrite and franckeite and, to a slightly lesser degree, to cannizzarite. The cylindrite structure comprises two layers, essentially isostructural with those in lengenbachite but half the thickness (Makovicky, 1974, 1976), a PbS-rich slab T two atomic layers thick ($1T$) and an O slab one octahedron thick ($1O$) (the latter slab similar to a slice of SnS_2). "Franckeite" forms a broad (chemical) solid-solution series based primarily on Pb^{2+}-Sn^{2+} substitution (Moh, 1984, 1986), and the family also comprises incaite (Makovicky, 1974, 1976) and the more recently discovered potosiite (Wolf et al., 1981) as well. Although there has been some doubt about the structures of various

[3] A copy of the atomic coordinates may be ordered as Document AM-88-390 from the Business Office, Mineralogical Society of America, 1625 I Street, N.W., Suite 414, Washington, D.C. 20006, U.S.A. Please remit $5.00 in advance for the microfiche.
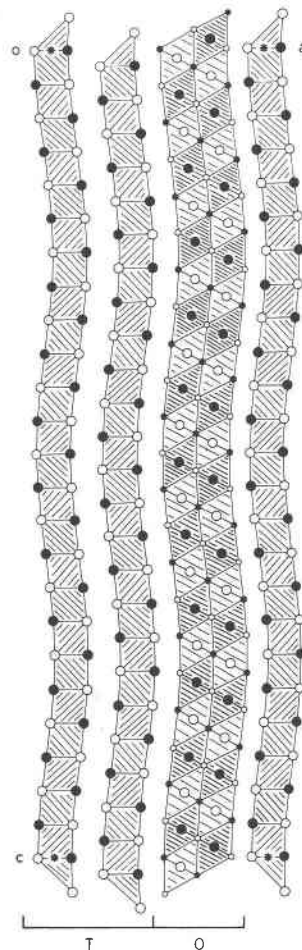
Fig. 6. Trial structure for lengenbachite. One unit cell is shown in the [010] projection, corresponding to the simulated structure image in Fig. 4. Layer type T contains (Pb,As) at $y = 0$ (open) and $y = \frac{1}{2}$ (filled) and S at $y = \frac{1}{4}$ (open) and $y = \frac{3}{4}$ (filled). Layer type O contains (As,Pb) (large circles) and S (small circles) at $y = 0, \frac{1}{3}, \frac{2}{3}$ (open) and $\frac{1}{6}, \frac{1}{2}, \frac{5}{6}$ (filled).

franckeites, it now seems clear that they possess the same crystal lattices and similar, semi- or incommensurable subcells (Mozgova et al., 1976; Williams and Hyde, 1988). High-resolution electron microscopy has recently shown (Williams and Hyde, 1988) that franckeite of typical composition has a one-octahedron-thick ($1O$) O slab similar to that in cylindrite, whereas the T layer is a structure four atomic layers thick ($2T$), almost isostructural with that suggested here for lengenbachite, but of approximately (Pb,Sn)S composition. In cannizzarite, approximately $Pb_{46}Bi_{54}S_{127}$, an O layer that is nearly isostructural with that in lengenbachite alternates with a $1T$ layer; however, the layers are rotated through $\pi/4$ from their relative orientations in the other minerals described above (Matzat, 1979). A three-octahedra (i.e., seven-atomic-layers-thick) O-layer ($3O$) synthetic cannizzarite variant has also been reported (Graham et al., 1953; Makovicky and Hyde, 1981). Together these complex minerals, which

cover an interesting and varied composition range, yet whose underlying structural principles are simple, form a homologous series with cylindrite, $1T:1O$, as one end member. The other known structures are cannizzarite, $1T:2O$, the synthetic cannizzarite variant, $1T:3O$, "franckeites," $2T:1O$, and lengenbachite, $2T:2O$.

Clearly, further refinement of the lengenbachite structure requires data, particularly HRTEM images, of higher resolution than those obtained to date. In particular, the roles of Ag and Cu, essential synthetic constituents (Rösch and Hellner, 1959), are not yet fully understood, although they are considered to be associated with the interlayer bonding and the corrugation. Further HRTEM work on this mineral is in progress to attempt to clarify the roles of Ag and Cu.

REFERENCES CITED

Graham, A.R., Thompson, R.M., and Berry, L.G. (1953) Studies of sulfosalts: XVII—Cannizzarite. American Mineralogist, 38, 536–544.

Holladay, A.C., and Eyring, L. (1986) A high-resolution electron microscopic study of some members of the vernier structural series $Ba_p(Fe_2S_4)_q$. Journal of Solid-State Chemistry, 64, 113–118.

Huchinson, A. (1907) The chemical composition of lengenbachite. Mineralogical Magazine, 14, 204–206.

Makovicky, E. (1974) Mineralogical data on cylindrite and incaite. Neues Jahrbuch für Mineralogie Monatshefte, 235–256.

——— (1976) Crystallography of cylindrite. Part 1. Crystal lattices of cylindrite and incaite. Neues Jahrbuch für Mineralogie Abhandlungen, 126, 304–326.

Makovicky, E., and Hyde, B.G. (1981) Non-commensurate (misfit) layer structures. Structure and Bonding, 46, 103–175.

Matzat, E. (1979) Cannizzarite. Acta Crystallographica, B35, 133–136.

Moh, G.H. (1984) Sulfosalts: Observations and mineral descriptions, experiments and applications. Neues Jahrbuch für Mineralogie Abhandlungen, 150, 25–64.

——— (1986) Current ore petrology: Microscopy, genesis, analyses and experimentation. Neues Jahrbuch für Mineralogie Abhandlungen, 153, 245–324.

Mozgova, N.N., Organova, N.I., and Gorshkov, A.I. (1976) Structural resemblance between incaite and franckeite. Doklady Akademii Nauk SSSR, Earth Sciences (English translation), 228, 110–113.

Nowacki, W. (1968) Uber hatchit, lengenbachit und verbait. Neues Jahrbuch für Mineralogie Monatshefte, 69–75.

Nuffield, E.W. (1944) Studies of mineral sulpho-salts: Lengenbachite. Transactions of the Royal Society of Canada, 3rd series, 38, section IV, 59–64.

Otero-Diaz, L., Fitz Gerald, J.D., Williams, T.B., and Hyde, B.G. (1985) On the monoclinic, binary-layer compound "LaCrS$_3$." Acta Crystallographica, B41, 405–410.

Rösch, H., and Hellner, E. (1959) Hydrothermale untersuchungen am system PbS-As_2S_3. Naturwiessenschaften, 46, 72.

Solly, R.H. (1905) Some new minerals from the Binnenthal, Switzerland. Mineralogical Magazine, 14, 72–82.

Thomas, J.M., Jefferson, D.A., Millinson, L.G., Smith, D.J., and Crawford, E.S. (1978) The elucidation of the structure of silicate minerals by high-resolution electron microscopy and X-ray emission microanalysis. Chemica Scripta, 14, 167–179.

Williams, T.B., and Hyde, B.G. (1988) Electron microscopy of cylindrite and franckeite. Physics and Chemistry of Minerals, 15, 521–544.

Wolf, M., Hunger, H.J., and Bewilogua, K. (1981) Potosiit—Ein neues Mineral des Kylindrit—Franckeit Gruppe. Freiberg Forschungsh, C364, 113–133.